Equivalent Current Density Reconstruction for Microwave Imaging Purposes

SALVATORE CAORSI, GIAN LUIGI GRAGNANI, AND MATTEO PASTORINO

Abstract—**The possibilities of reconstructing the distribution of the equivalent current density vector in a domain with a known volume, V, inside which dielectric scatterers stand at arbitrary locations, are studied by means of numerical computer simulations. An integrodifferential formulation of the three-dimensional electromagnetic inverse scattering is transformed into matrix form through the application of the moment method. A pseudoinversion algorithm overcoming ill-conditioned problems is used to obtain the distribution of the equivalent current density also in the case where the input data (i.e., the simulated values of the scattered field vector to be obtained in an observation domain) are affected either by Gaussian noise or by uniformly distributed errors. The results furnish information that could be used to devise a possible imaging method for detecting the locations and surface shapes of scattering objects.**

I. Introduction

IN RECENT YEARS, there has been a growing interest in the capabilities of microwave imaging as a technique for determining the dielectric permittivity distribution in inhomogeneous materials. Some works [1]–[5] have been developed on the basis of the so-called Fourier diffraction projection theorem [1], which is the basis for diffraction tomography, and have been successfully applied in the case of weakly scattering inhomogeneities. To study weak electromagnetic scattering, some approximations can be used, such as those of Born and Rytov, and some techniques have been devised which resemble the classic back-projection methods [6], [7]. In some works, in order to deal with strongly scattering objects, the moment method [8] was used to develop algorithms for deducing the dielectric characteristics of inhomogeneous bodies with two-dimensional [9] and three-dimensional geometries [10]. In particular, the work by Guo and Guo [11] provides an extensive theory for this kind of algorithm.

In the present work, by following the procedure presented in [11], we want to study the possibilities of reconstructing the distribution of the equivalent current density vector in a domain, called the investigation domain (inside which unknown dielectric scatterers can be placed at arbitrary positions), on the basis of the knowledge of the scattered electric field vector in a domain (external to the investigation one) called the observation domain.

The purpose of this study is to obtain useful information for deriving a possible imaging method which, instead of determining the dielectric permittivity, provides the locations and surface shapes of unknown objects in a space region with an *a priori* known volume (investigation domain). To this end, the reconstruction is obtained, in a three-dimensional geometry, by a numerical approach based on the application of the moment method to the inverse electromagnetic scattering equations and on a pseudoinversion algorithm for the solution of the corresponding linear system of algebraic equations. Special attention should be devoted to those zones of the investigation volume where the value of the reconstructed equivalent current density becomes equal to zero, since this situation does not directly prove the presence or the absence of scattering objects in those zones, unless information is provided about the values of the electric field vector at the points where the current density vanishes.

Finally, a number of numerical computer simulations have been performed even in the case where the input data (which are represented by the components of the electromagnetic field vectors measured in a region external to the investigation one) are affected by noise levels corresponding to low values of the signal-to-noise ratio or by significant measurement errors.

II. Mathematical Formulation

In this section, an electromagnetic scattering formulation in terms of the electric field vector [11] is used to determine the distribution of the equivalent current density vector inside an investigation domain when the scattered electric field vector in an external observation domain is known. The investigation domain has known volume, V, and is immersed in a homogeneous dissipative medium with a dielectric permittivity ϵ_e, an electric conductivity σ_e, and a relative magnetic permeability equal to 1.

If the volume V is exposed to an electromagnetic source producing an incident electric field vector $\boldsymbol{E}_{\text{inc}}(\boldsymbol{r})$, under the assumption that the mutual coupling is negligible, the total electric field vector $\boldsymbol{E}_{\text{tot}}(\boldsymbol{r})$ at any point $\boldsymbol{r}$, in particular, inside the observation domain D, can be expressed as follows:

$$\boldsymbol{E}_{\text{tot}}(\boldsymbol{r}) = \boldsymbol{E}_{\text{inc}}(\boldsymbol{r}) - \boldsymbol{E}_{\text{scatt}}(\boldsymbol{r}) \tag{1}$$

where $\boldsymbol{E}_{\text{scatt}}(\boldsymbol{r})$ is the scattered electric field vector due to the dielectric properties of possible scattering objects present inside V. Under these conditions, the total electric field

Manuscript received July 29, 1987, revised December 12, 1988

The authors are with the Department of Biophysical and Electronic Engineering, University of Genoa, Via all'Opera Pia, 11a, 16145 Genoa, Italy.

IEEE Log Number 8926573.

vector outside the investigation volume V satisfies the vector wave equation:

$$\nabla \times \nabla \times \boldsymbol{E}_{\text{tot}}(\boldsymbol{r}) - k_e^2 \boldsymbol{E}_{\text{tot}}(\boldsymbol{r}) = 0, \qquad \boldsymbol{r} \notin V \quad (2)$$

whereas inside the investigation volume V, the following relation holds:

$$\nabla \times \nabla \times \boldsymbol{E}_{\text{tot}}(\boldsymbol{r}) - k_V^2(\boldsymbol{r}) \boldsymbol{E}_{\text{tot}}(\boldsymbol{r}) = 0, \qquad \boldsymbol{r} \in V \quad (3)$$

where k_e and $k_V(\boldsymbol{r})$ represent the wavenumbers outside and inside the investigation volume V, respectively, and the notation "$\nabla \times$" stands for the curl operation.

If we now substitute relation (1) into both (2) and (3), and recall that

$$\nabla \times \nabla \times \boldsymbol{E}_{\text{inc}}(\boldsymbol{r}) - k_e^2 \boldsymbol{E}_{\text{inc}}(\boldsymbol{r}) = 0 \quad (4)$$

everywhere, we obtain, after a few trivial steps, the following relationships:

$$\nabla \times \nabla \times \boldsymbol{E}_{\text{scatt}}(\boldsymbol{r}) - k_e^2 \boldsymbol{E}_{\text{scatt}}(\boldsymbol{r}) = 0, \qquad \boldsymbol{r} \notin V \quad (5)$$

$$\nabla \times \nabla \times \boldsymbol{E}_{\text{scatt}}(\boldsymbol{r}) - k_e^2 \boldsymbol{E}_{\text{scatt}}(\boldsymbol{r}) = \left(k_V^2(\boldsymbol{r}) - k_e^2\right) \boldsymbol{E}_{\text{tot}}(\boldsymbol{r}), \qquad \boldsymbol{r} \in V. \quad (6)$$

By introducing an equivalent current density $\boldsymbol{J}_{\text{eq}}$, (6) can be rewritten as follows:

$$\nabla \times \nabla \times \boldsymbol{E}_{\text{scatt}}(\boldsymbol{r}) - k_e^2 \boldsymbol{E}_{\text{scatt}}(\boldsymbol{r}) = -j\omega\mu_0 \boldsymbol{J}_{\text{eq}}(\boldsymbol{r}) \quad (7)$$

where

$$\boldsymbol{J}_{\text{eq}}(\boldsymbol{r}) = \frac{j}{\omega\mu_0}\left(k_V^2(\boldsymbol{r}) - k_e^2\right) \boldsymbol{E}_{\text{tot}}(\boldsymbol{r}) \quad (8)$$

and

$$\frac{j}{\omega\mu_0}\left(k_V^2(\boldsymbol{r}) - k_e^2\right) = \left(\sigma(\boldsymbol{r}) - \sigma_e\right) + j\omega\left(\epsilon(\boldsymbol{r}) - \epsilon_e\right). \quad (9)$$

In this way, by means of (5) and (7), the problem of representing the possible presence of scattering inhomogeneities inside the investigation volume V has been transformed into a field–source problem in a homogeneous medium.

It is worth noting that, if $\epsilon(\boldsymbol{r}) = \epsilon_e$ and $\sigma(\boldsymbol{r}) = \sigma_e$, we have $\boldsymbol{J}_{\text{eq}}(\boldsymbol{r}) = 0$. Unfortunately, while $\boldsymbol{J}_{\text{eq}}(\boldsymbol{r}) \neq 0$ is a sufficient condition to state the presence of scattering objects, $\boldsymbol{J}_{\text{eq}}(\boldsymbol{r}) = 0$ is only a necessary, not a sufficient, condition to prove the absence of inhomogeneities. To this end, the knowledge of the total electric field vector at the points $\boldsymbol{r}^*$ where $\boldsymbol{J}_{\text{eq}}(\boldsymbol{r}^*) = 0$ can be determinant. In fact, if $\boldsymbol{E}_{\text{tot}}(\boldsymbol{r}^*) \neq 0$, then the situation $\boldsymbol{J}_{\text{eq}}(\boldsymbol{r}^*) = 0$ becomes a necessary and sufficient condition to state that the dielectric characteristics of $\boldsymbol{r}^*$, under the assumption of finite material properties, are equal to those of the external surrounding medium. On the contrary, if $\boldsymbol{E}_{\text{tot}}(\boldsymbol{r}^*) = 0$, nothing can be deduced about the nature of the material at $\boldsymbol{r}^*$, and information can be obtained through a limiting operation.

In other words, the points inside the investigation volume, V, where $\boldsymbol{J}_{\text{eq}}(\boldsymbol{r}) \neq 0$ represent inhomogeneities; that is, they indicate the presence of scattering objects, while the points whose dielectric properties equal those of the outside medium can be modeled with a null equivalent current density vector. However, care must be exercised in considering the points where both the equivalent current density vector and the total electric field vector become equal to zero.

As is well known, the scattered electric field vector as a solution to (7), under Sommerfeld's radiation conditions [12], can be written as follows:

$$\boldsymbol{E}_{\text{scatt}}(\boldsymbol{r}) = \int_V \boldsymbol{J}_{\text{eq}}(\boldsymbol{r}') \cdot \bar{\bar{G}}(\boldsymbol{r}/\boldsymbol{r}')\, d\boldsymbol{r}' \quad (10)$$

where $\bar{\bar{G}}(\boldsymbol{r}/\boldsymbol{r}')$ is Green's well-known dyadic function for free space [13], [14]. Application of the moment method [8] to (10) allows us to determine the equivalent current density vector at a finite number of points inside the investigation volume, on the basis of the knowledge of the scattered electric field vector at a finite number M of points inside the observation domain D. To this end, let us represent the equivalent current density vector as a sum of subsectional rectangular basis functions, as follows:

$$\boldsymbol{j}_{\text{eq}}(\boldsymbol{r}) = \sum_1^N {}_n \boldsymbol{J}_n. \quad (11)$$

This amounts to subdividing the investigation volume V into N subvolumes, and to assuming that $\boldsymbol{J}_n$ is constant in the related subvolume and equal to 0 elsewhere. Furthermore, if we use a finite number M of Dirac's delta as weighting functions for the observation domain D, we obtain, starting from (10),

$$\boldsymbol{E}_{\text{scatt}}(\boldsymbol{r}_m) = \sum_1^N {}_n \int_{V_n} \boldsymbol{J}_n \cdot \bar{\bar{G}}(\boldsymbol{r}_m/\boldsymbol{r}_n')\, d\boldsymbol{r}_n', \qquad m = 1, \cdots, M \quad (12)$$

where $\boldsymbol{r}_m$ is the mth point inside the observation domain D.

In this way, the integral equation (10) is transformed into relation (12), which represents a linear system of $3M$ algebraic equations with $3N$ unknowns. In fact, in this system the unknown terms are the three Cartesian components of the equivalent current density vector, $\boldsymbol{J}_n$, for each of the N subvolumes of the investigation volume:

$$[J] = \left\{ \boldsymbol{J}_{n_p}; \quad p = x, y, z; \quad n = 1, \cdots, N \right\} \quad (13)$$

while the known terms are the three Cartesian components of the scattered electric field vector, $\boldsymbol{E}_{\text{scatt}}(\boldsymbol{r}_m)$, for each of the M points $\boldsymbol{r}_m$ of the observation domain:

$$[e_{\text{scatt}}] = \left\{ \boldsymbol{E}_{\text{scatt}_p}(\boldsymbol{r}_m); \quad p = x, y, z; \quad m = 1, \cdots, M \right\}. \quad (14)$$

In accordance with relation (1), these components can be obtained, in the observation domain, by subtracting the components of the incident electric field vector from those of the total electric field vector.

Relation (12) can be rewritten in matrix form:

$$[G][J] = [e_{\text{scatt}}] \quad (15)$$

where the matrix of the coefficients, $[G]$, is obtained by

calculating numerically the Cartesian components of the integral appearing in (12) for each subvolume V_n and each point r_m.

In the present paper, the solution of (15) is obtained by using a pseudoinversion algorithm [15], [16] of matrix $[G]$, which, besides being useful to rectangular linear systems, can overcome ill-conditioned problems [17]. In fact, application of such a pseudoinversion algorithm, based on the Gram–Schmidt orthogonalization procedure, allows one to obtain such a solution to system (13) whereby the following norms:

$$\|[G][J]-[e_{\text{scatt}}]\| \quad \text{and} \quad \|[J]\| \tag{16}$$

are simultaneously minimized.

As is known, this minimization process allows one to avoid errors that are caused by numerical instabilities due to the inverse scattering formulation [9], [18], [19].

Therefore, the distribution of the Cartesian components of the equivalent current density vector $[J]$ inside the discretized investigation volume is given by

$$[J]=[G]^{+}[e_{\text{scatt}}] \tag{17}$$

where $[G]^{+}$ represents the pseudoinverse matrix obtained by using the above-mentioned algorithm.

On the basis of relation (17), we can assess the possibilities of detecting the presence and the surface shapes of scattering objects inside the investigation volume V.

As stated above, an imaging procedure based on relation (17) may be implemented, provided that the value of the total electric field is taken into account where the equivalent current density vanishes. Moreover, from a numerical standpoint, since the calculated values of J_n may be very small, the introduction of appropriate thresholds to discriminate the empty cells from the full ones would again pose the problem of testing the total electric field vector for the empty cells. We are currently developing a microwave imaging method that, as an extension of the formulation used in this paper and on the basis of the above considerations, allows us not only to localize but also to perform the dielectric permittivity reconstruction by resorting, where both $J_{\text{eq}}=0$ and $E_{\text{tot}}=0$, to a numerical limiting operation in an appropriate iterative way, until the spatial resolution imposed by the actual noise characteristics is reached.

III. Numerical Examples

In this section, we report the results of several numerical examples in which the presence of dielectric objects inside the investigation volume, exposed to incident electromagnetic waves, has been simulated by means of idealized scatterers consisting in suitable equivalent current density distributions.

In the first example, a scatterer of cubic shape, simulated by a unit equivalent current density vector with uniform spatial distribution, has been placed in a λ_0-sided investigation volume partitioned into 27 cubic subvolumes (Fig. 1); in the example, the scatterer occupies one whole subvolume (the 22nd). The observation domain is made up

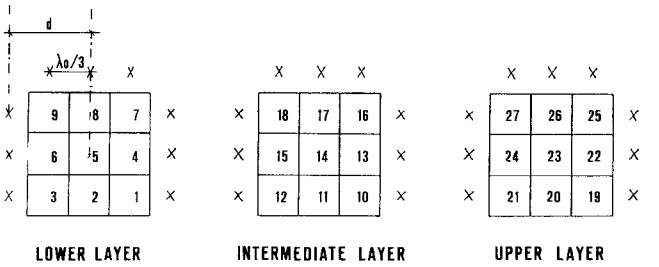

Fig. 1. The cell numbering for the three-layered cubic investigation volume (27 cells) and the positions of the observation points (27 points marked with crosses).

of 27 equally spaced measurement points ($\lambda_0/3$) (the points marked with crosses in Fig. 1) on three planes, each parallel to one face of the investigation volume. As no analytic relationship is available, the values of the components of the scattered electric field vector in the observation domain have been obtained by numerically solving the equation of the direct scattering problem. It is worth noting that, in this way, the values of the scattered electric field may be affected by errors due to the slow convergence of the computation.

The above arrangement has turned out to be more suited to obtaining significant results than other arrangements, in which the measurement points are arranged on only one of the three planes. In fact, such an arrangement allows an acceptable reconstruction of the equivalent current density, even for distance values of the observation domain to the center of the investigation volume that are equal to some wavelengths; instead, other arrangements have resulted in less accurate reconstructions for distance values greater than λ_0. This confirms the fact that a better spatial resolution is usually obtained when the input data are recorded over a large solid angle.

In the case in which the distance of the observation domain to the center of the investigation volume was assumed to be equal to λ_0, we obtained a reconstruction of the amplitude of the equivalent current density in the 22nd cell containing the scatterer with an error less than 0.01 percent. The results on the remaining cells, where a null current density is expected (empty cells), are illustrated in Fig. 2. This figure shows the number of subvolumes for which the normalized values of the amplitude of the current density vector (which are expressed as percent values of the original value of the 22nd cell) are included in the values of the corresponding interval on the axis of abscissas. In this figure, as well as in the following ones, $|J_i|$ and $|\tilde{J}_i|$ stand for the original and calculated amplitudes of the current densities in the ith cell, respectively.

In order to evaluate the effects of a scatterer's location inside the investigation volume, the equivalent current density has been reconstructed by making the scatterer coincide with successive different subvolumes. Fig. 3 shows the global results of this simulation, concerning the normalized current values in the empty cells (27×26 cells). This figure provides important information about the probability of wrong localizations or of incorrect defini-

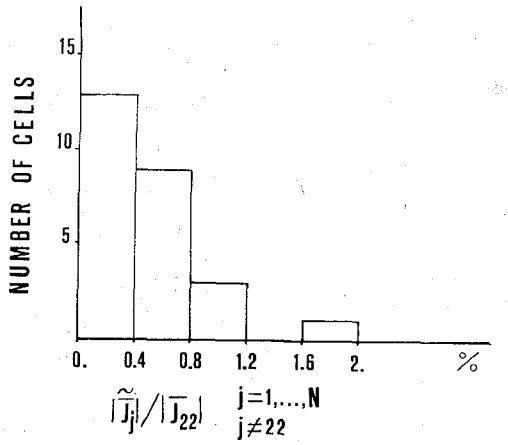

Fig. 2. Number of empty cells for which the normalized values of the amplitude of the current density vector (which are expressed as percent values of the original value of the 22nd cell) are included in the values of the corresponding interval on the axis of abscissas (first simulation case).

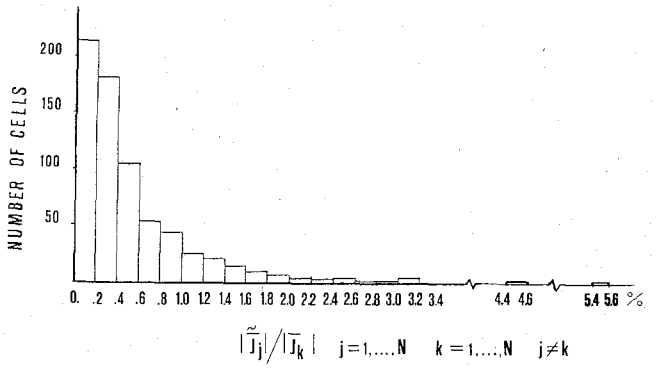

Fig. 3. Global results for the normalized values of the amplitude of the current density in the empty cells (27×26 cells) when the location of the scatterer coincides with successive different subvolumes.

tions of the contour surfaces. In each simulation, the error percentages regarding the reconstruction in a subvolume containing a scatterer have been found to be less than 0.95 percent, and the worst case has turned out to be the one in which the scatterer is located in the 11th cell.

Both the effects of realistic errors concerning the components of the scattered electric field vector and those of significant levels of additive Gaussian noise have been assessed. To this end, the input data for the reconstruction process have been modified by adding random error arrays with uniform distributions between $-w$ and w (w being the maximum error percentage for the calculated electric field) or with Gaussian distributions; such errors were related to different values of the signal-to-noise ratio, S/N. The normalized values of the equivalent current density in the empty cells, obtained by these two sets of simulations, are shown in Figs. 4 and 5, respectively. It is worth noting how large w values correspond to low values of the S/N ratio; for instance, $w=5$ corresponds to $S/N=$ about 20 dB, and $w=20$ corresponds to $S/N=$ about 6 dB.

Other computer simulations have been performed considering the presence of more scatterers. In particular, in

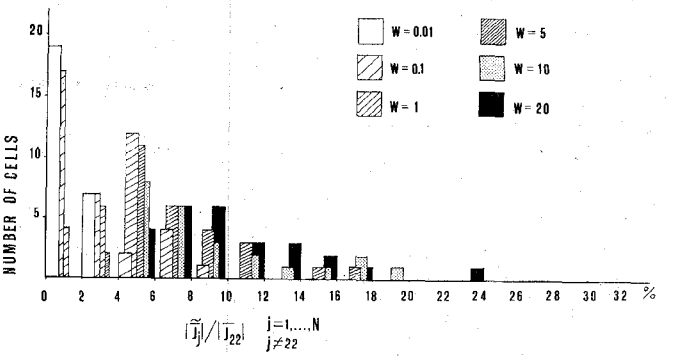

Fig. 4. Effects of random measurement errors characterized by a uniform distribution (between $-w$ and w percent of the calculated electric field) on the normalized values of the reconstructed amplitude of the current density vector in the empty cells.

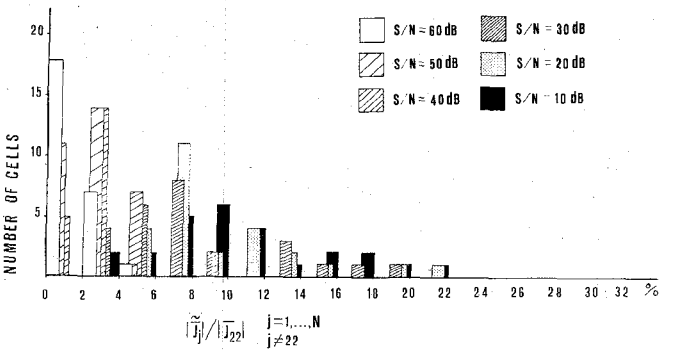

Fig. 5. Effects of Gaussian noise on the normalized values of the reconstructed amplitude of the current density vector in the empty cells.

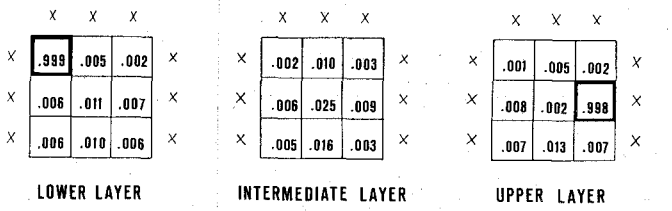

Fig. 6. Values of the normalized amplitude of the equivalent current density vector, reconstructed in the three layers of the investigation volume. The cells containing scatterers are the ninth and the 22nd.

the same investigation volume, two idealized scatterers have been placed as in the previous simulations. Fig. 6 shows the values of the amplitude of the equivalent current density vector, reconstructed in the three layers of the investigation volume, for the case where the cells containing scatterers are the ninth and the 22nd. The locations of the two scatterers have then been varied, until $\binom{27}{2}$ possible combinations have been considered. In each case, the maximum error in the reconstruction of the equivalent current density vector for the cell containing scatterers has turned out to be less than 1.0 percent. Fig. 7 shows the normalized percent values of the equivalent current in the empty cells (in total, $\binom{27}{2}\times 25$ cells). Of the $\binom{27}{2}$ possible combinations, the best results have been obtained in the case where the scatterers occupied the 12th and 19th cells

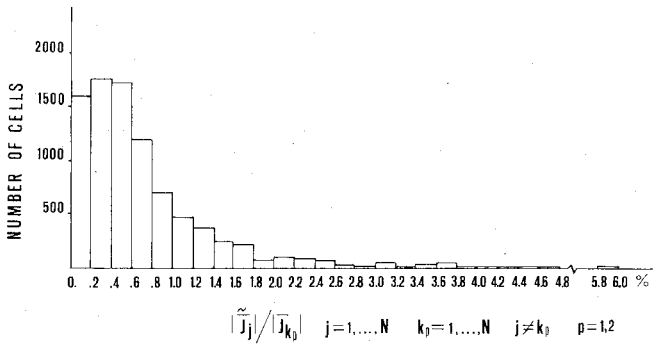

Fig. 7. Global results for the normalized values of the amplitude of the current density in the empty cells when the locations of the two scatterers coincide with successive different subvolumes (total number of empty cells: $\binom{27}{2} \times 25$).

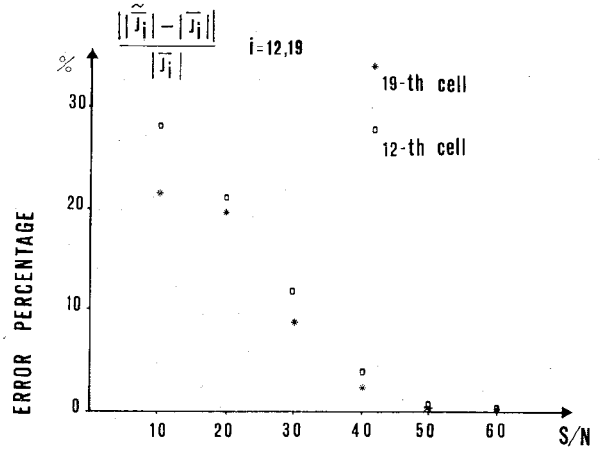

Fig. 8. Error percentage related to the reconstruction of the equivalent current density vector in the 12th and 19th cells in the case of additive Gaussian noise.

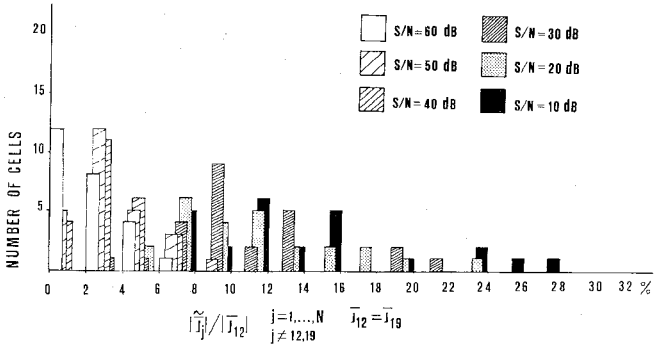

Fig. 9. Effects of Gaussian noise on the normalized values of the reconstructed amplitude of the current density vector in the empty cells in the case where the cells containing scatterers are the 12th and 19th.

or for configurations symmetrical with the present one in terms of the problem geometry.

The error percentage related to the reconstruction of the equivalent current density vector in the 12th and 19th cells is shown in Fig. 8 for the case of additive Gaussian noise. Fig. 9 gives the normalized percent values of the equivalent current density in the empty cells, in the same case as in Fig. 8.

The configuration that has yielded the worst results is the one in which the two scatterers occupy the seventh and

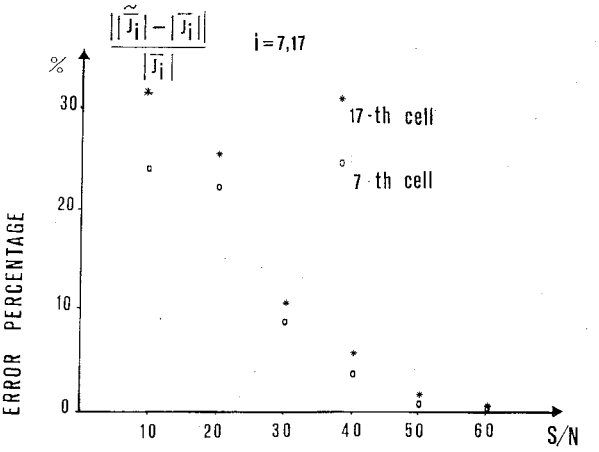

Fig. 10. Error percentage related to the reconstruction of the equivalent current density vector in the seventh and 17th cells in the case of additive Gaussian noise.

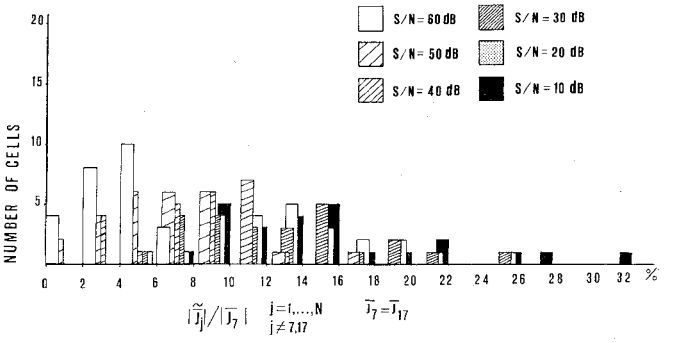

Fig. 11. Effects of Gaussian noise on the normalized value of the reconstructed amplitude of the current density vector in the empty cells in the case where the cells containing scatterers are the seventh and 17th.

17th cells (as well as other configurations symmetrical with this one). Fig. 10 gives the results of the reconstruction in the cells containing the scatterers, in the case of Gaussian noise. Fig. 11 gives the reconstruction errors for the empty cells, in the same case.

To assess the possibility that, in a particular cell, the error may accumulate to a much greater value when more scattering objects are present inside the investigation volume, further studies have been made simulating this specific situation. Even in the case of incorrect data, the results have shown a negligible error in the reconstruction of the scatterer and a slight increase in the normalized current values in the empty cells. Fig. 12 illustrates the normalized current values in the case of five scatterers.

Finally, in other numerical simulations, an investigation volume measuring $(5\lambda_0)^3$, partitioned into 27 cubic cells, has been considered. A scatterer, equal to those previously utilized, has been placed in the center of the 22nd cell. The observation domain was made up of 27 points arranged as those considered in the previous simulations. The distance between the observation domain and the center of the investigation volume was $8/3\lambda_0$.

The effects of Gaussian noise on the reconstruction of the scatterer are shown in Fig. 13. Fig. 14 shows the results relevant to the empty cells. Figs. 15 and 16 present the

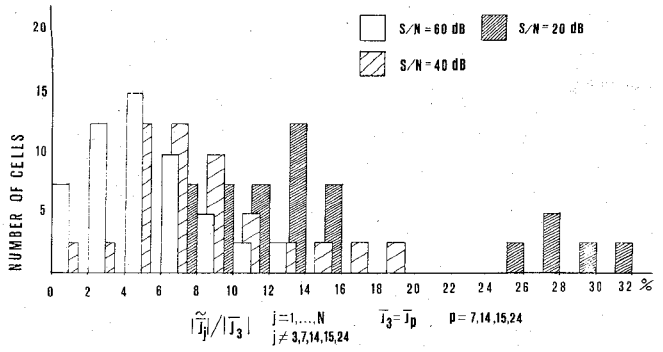

Fig. 12. The normalized values of the amplitude of the reconstructed current density vector are included in the values of the corresponding interval on the axis of abscissas in the case of five scatterers.

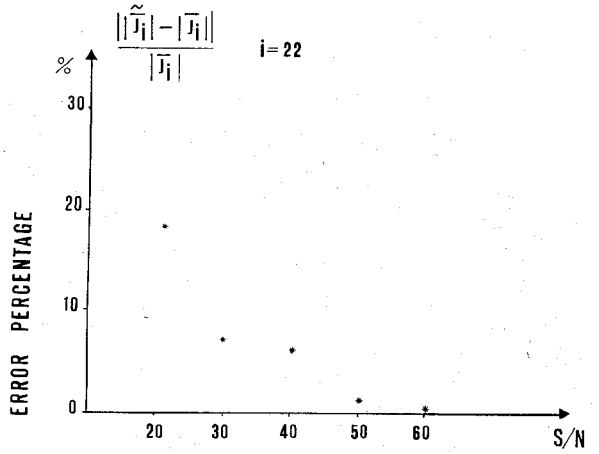

Fig. 13. Error percentage related to the reconstruction of the equivalent current density vector in the 22nd cell of the $(5\lambda_0)^3$ investigation volume in the case of additive Gaussian noise.

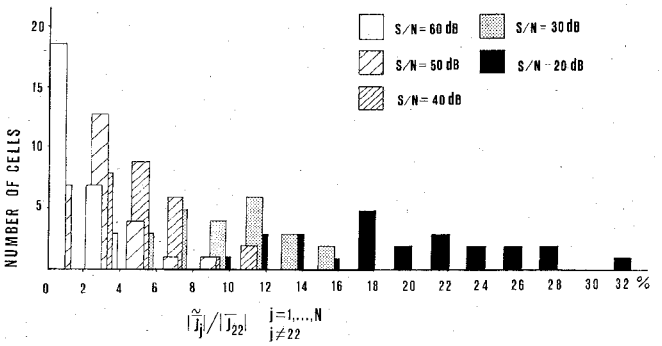

Fig. 14. Effects of Gaussian noise on the normalized values of the reconstructed amplitude of the current density vector in the empty cells in the case of a $(5\lambda_0)^3$ investigation volume.

results obtained in the case of a uniform error introduced into the input data. It should be noted that, as the scatterer's dimensions are smaller than those of the discretization volume, one can expect to reconstruct, inside the 22nd cell, an average equivalent current density with a vector equal to 1/125, as compared with the original current density.

IV. Conclusions

In this paper, a widely known approach to electromagnetic inverse scattering has been employed to determine the distribution of the equivalent current density vector in

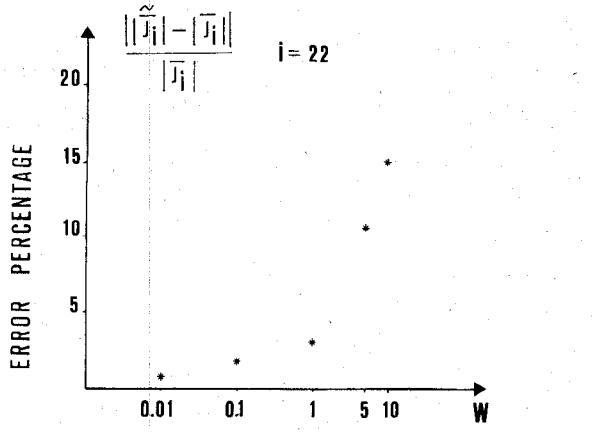

Fig. 15. Error percentage related to the reconstruction of the equivalent current density vector in the 22nd cell of the $(5\lambda_0)^3$ investigation volume in the case of a uniformly distributed error.

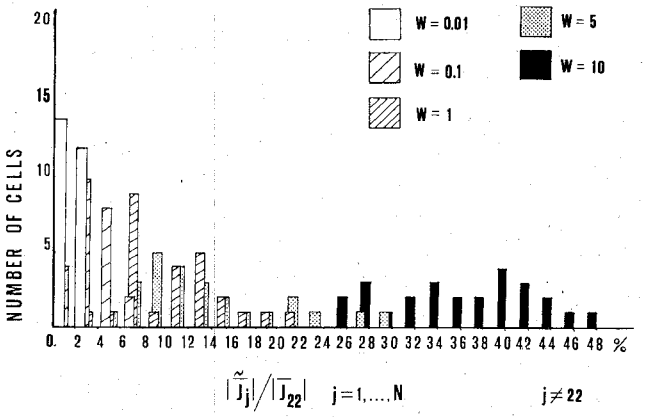

Fig. 16. Effects of a uniformly distributed error on the normalized values of the reconstructed amplitude of the current density vector in the empty cells in the case of a $(5\lambda_0)^3$ investigation volume.

a three-dimensional geometry. The moment method has been applied to transform the integrodifferential formulation into matrix form, which has been solved by using a pseudoinversion algorithm to overcome ill-conditioned problems. By means of this numerical technique, we have been able to assess the possibilities of reconstructing the equivalent current density introduced by the presence of dielectric objects inside an investigation domain with an *a priori* known volume V.

Numerical simulations have been performed using *a priori* known values of the equivalent current density, and starting from the calculated values of the scattered electric field vector also in the case where the input data were affected by Gaussian noise or by uniformly distributed errors.

The results of the computer simulations are satisfactory and provide useful information for developing a microwave imaging method for detecting the presence and the surface shapes of unknown dielectric objects, provided that particular care is exercised in those critical situations where both the equivalent current and the total electric field become equal to zero. In a work under current development, where we deal also with dielectric permittivity reconstruction, we suggest performing, in such critical

cases, a numerical limiting operation until the required spatial resolution values are reached.

REFERENCES

[1] A. J. Devaney, "Reconstructive tomography with diffracting wavefields," *Inverse Problems*, vol. 2, pp. 161–183, 1986.

[2] C. Pichot, L. Jofre, G. Peronnet, and J. C. Bolomey, "Active microwave imaging of inhomogeneous bodies," *IEEE Trans. Antennas Propagat.*, vol. AP-33, pp. 416–425, 1985.

[3] M. Slaney, A. C. Kak, and L. E. Larsen, "Limitation of imaging with first-order diffraction tomography," *IEEE Trans. Microwave Theory Tech.*, vol. MTT-32, pp. 860–873, 1984.

[4] A. J. Devaney, "Geophysical diffraction tomography," *IEEE Trans. Geosci. Remote Sensing*, vol. GE-22, pp. 3–13, 1984.

[5] J. M. Harris, "Diffraction tomography with arrays of discrete sources and receivers," *IEEE Trans. Geosci. Remote Sensing*, vol. GE-25, pp. 448–455, 1987.

[6] J. A. Devaney, "A filtered backpropagation algorithm for diffraction tomography," *Ultrasonic Imaging*, vol. 4, pp. 336–350, 1982.

[7] K. I. Schultz and D. L. Jaggard, "Microwave projection imaging for refractive objects: A new method," *J. Opt. Soc. Amer.*, vol. 4, pp. 1773–1782, 1987.

[8] R. F. Harrington, *Field Computation by Moment Method*. New York: Macmillan, 1968.

[9] M. M. Ney, A. M. Smith, and S. S. Stuchly, "A solution of electromagnetic imaging using pseudoinverse transformation," *IEEE Trans. Med. Imaging*, vol MI-3, pp. 155–162, 1984.

[10] D. K. Ghodgaonkar, O. P. Gandhi, and M. J. Hagmann, "Estimation of complex permittivities of three-dimensional inhomogeneous biological bodies," *IEEE Trans. Microwave Theory Tech.*, vol. MTT-22, pp. 1273–1280, 1974.

[11] T. C. Guo and W. W. Guo, "Physics of image formation by microwave scattering," *SPIE Proc.*, vol. 767, 1987.

[12] D. S. Jones, *The Theory of Electromagnetism*. Oxford: Pergamon, 1964.

[13] C. T. Tai, *Dyadic Green's Functions in Electromagnetic Theory*. Scranton: International Textbook, 1971.

[14] J. Van Bladel, "Some remarks on Green's dyadic for infinite space," *IRE Trans. Antennas Propagat.*, vol AP-9, pp. 563–566, 1961.

[15] R. Penrose, "A generalized inverse for matrices," *Proc. Cambridge Phil. Soc.*, vol. 51, pp. 406–413, 1955.

[16] M. M. Ney, "Method of moments as applied to electromagnetic problems," *IEEE Trans. Microwave Theory Tech.*, vol. MTT-33, pp. 972–980, 1985.

[17] T. Sarkar, D. D. Weiner, and V. K. Jain, "Some mathematical considerations in dealing with the inverse problem," *IEEE Trans. Antennas Propagat.*, vol. AP-29, pp. 373–379, 1981.

[18] R. P. Porter and A. J. Devaney, "Holography and the inverse source problem," *J. Opt. Soc. Amer.*, vol. 72, pp. 327–330, 1982.

[19] W. R. Stone, "A review and examination of results on uniqueness in inverse problems," *Radio Sci.*, vol. 22, pp. 1026–1030, 1987.

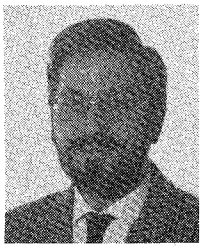

Salvatore Caorsi received the "laurea" degree in electronic engineering in 1973 from the University of Genoa, Genoa, Italy, and then worked at this university as a researcher.

Since 1976, he has been Professor of Antennas and Propagation there, and in 1985 he also assumed the title of Professor of Fundamentals of Active Remote Sensing. He is with the Department of Biophysical and Electronic Engineering, where he is responsible for the Applied Electromagnetism Group and for the Research Center on the Interactions between Electromagnetic Fields and Biological Systems (IEMBS). His primary research activities are focused on applications of electromagnetic fields to telecommunications, artificial vision and remote sensing, biology, and medicine. In particular, he is working on research projects concerning microwave hyperthermia and radiometry in oncological therapy; numerical methods for solving electromagnetic problems; and inverse scattering and microwave imaging.

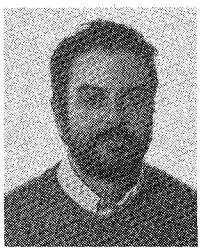

Gian Luigi Gragnani received the "laurea" degree in electronic engineering from the University of Genoa, Genoa, Italy, in 1985.

In the same year he joined the Applied Electromagnetism Group in the Department of Biophysical and Electronic Engineering. His main interests are in the area of electromagnetic scattering, both direct and inverse, and in numerical methods for addressing electromagnetic problems. In addition, he is now doing research work on electromagnetic compatibility.

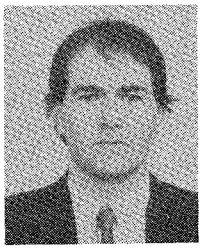

Matteo Pastorino is a Ph.D. student of electronics and computer science in the Department of Biophysical and Electronic Engineering, University of Genoa, Genoa, Italy. He received the "laurea" degree in electronic engineering from the University of Genoa in 1987. Since that year, he has cooperated in the activities of the Applied Electromagnetism Group. His main interests are in the field of electromagnetic direct and inverse scattering, microwave imaging, wave propagation in the presence of nonlinear media, and numerical methods in electromagnetism.